EUROPHYSICS LETTERS 1 April 1993

Europhys. Lett., **22** (1), pp. 17-22 (1993)

Transition to Chaos by Spatio-Temporal Intermittency in Directional Viscous Fingering.

S. MICHALLAND, M. RABAUD and Y. COUDER

Laboratoire de Physique Statistique, Ecole Normale Supérieure
associé au CNRS et aux Universités Paris VI et VII
24 rue Lhomond, 75231 Paris Cedex 05, France

(received 30 October 1992; accepted in final form 29 January 1993)

PACS. 47.20 – Hydrodynamic stability and instability.

Abstract. – We present a statistical description of the transition to chaos in a directional viscous fingering experiment. In this extended one-dimensional system the order-disorder transition follows a scenario of spatio-temporal intermittency and appears as a second-order transition. The critical exponents of the transition are determined and compared with other systems exhibiting a similar behaviour. The values of these exponents are discussed.

During the last few years, important experimental and theoretical studies have been focused on extended one-dimensional (1D) dynamical systems [1] in order to analyse complex behaviours such as the transition to chaos. Numerical simulations of coupled map lattices [2] or of damped Kuramoto-Sivashinski equations [3] have revealed that in such 1D systems the transition between an ordered state and a fully disordered one can occur via Spatio-Temporal Intermittency (STI). The STI is characterised by the coexistence in time and space of chaotic areas with regular ones. This has also been observed in experiments of confined convection and in the forcing of a linear array of vortices [4] and directional viscous fingering [5, 6]. Statistical studies performed in ref. [2-4] suggested that the STI transition to chaos behaves as a second-order transition but the question remained whether or not the STI transitions belong to the same universality class. We present in this letter a statistical study of the STI transition to chaos observed in directional viscous fingering, the local dynamics and contamination processes of which have been described in ref. [6].

Directional viscous fingering is an instability which affects the meniscus of a viscous fluid placed in the widening gap between two moving solid surfaces [7]. It occurs often in the coating processes, a context where it is called the ribbing instability and in which it has been widely investigated [8]. Revisiting this instability in a new configuration which allowed to visualise the interface, we found [5] that the velocity of the two walls formed two independent control parameters governing the non-linear dynamics of the instability and in particular the transition to chaos hereafter presented.

The experimental set-up is composed of two horizontal glass cylinders, one inside the other (of diameter, respectively, 66 and 100 mm and length 380 and 420 mm). These cylinders are off-centred and the minimum spacing b_0 between them has been adjusted to

(0.370 ± 0.015) mm. A small amount of silicone oil is introduced in the system and fills the gap at the bottom. As the oil wets the glass, two oil films coat the rotating cylinders. We study the shape of the meniscus parallel to the cylinders' axis. Two capillary numbers of the type $Ca = \mu V/T$ can be defined, where μ is the oil dynamical viscosity and T the interfacial tension. In these numbers Ca_i and Ca_e, V is V_i or V_e, the velocities of the inner or outer cylinders, respectively. Ca_i and Ca_e are the two control parameters of the experiment.

One of the menisci between air and oil, originally linear and parallel to the axes, becomes unstable when the cylinders rotate fast enough. The threshold depends on the geometry of the cell (*i.e.* b_0 and the radii of the cylinders) an on the two capillary numbers. The value of this threshold has been described elsewhere [5, 7] together with the various dynamical regimes. We will just summarise the possible dynamics:

With one cylinder at rest, the unstable interface is formed by a periodic pattern of steady cells. These cells are sinusoidal near threshold, deep and similar to Saffman-Taylor fingers far from it [9].

When the two cylinders are rotating, after a first threshold giving rise to the static pattern above described, the interface becomes time dependent. In the case of counter-rotating cylinders, this state is propagative with parity symmetry breaking [10]. In the case of corotating cylinders, the system evolves to chaotic dynamics which is characterised by a loss of spatial and temporal coherence of the cellular pattern.

In this letter we focus on the statistical analysis of the transition between the regular state and the chaotic one. To study this transition we fixed the inner capillary number Ca_i at a constant value above threshold, the interface thus being a static array of deep cells. Then we set the outer cylinder into corotation. Our control parameter for the transition to chaos is therefore the capillary number Ca_e. Most of the results presented here have been obtained for constant $Ca_i = 3$ (in a geometry for which the first instability appears for a single rotating cylinder at a critical value $Ca = 0.371$). The front is formed of approximately 60 deep cells. The phase defects occurring during transients [11] or in the weakly chaotic regime [6] are either dilatation waves propagating along the front as in the classical directional growth [12] or defects formed of a pair of two non-propagating larger cells. We first present the results for $Ca_i = 3$ and we will compare them with the results of a similar transition obtained at a lower Ca_i value.

When the control parameter Ca_e is zero (fixed outer cylinder), the interface is formed by the regular and static cellular pattern. The wavelength λ of the pattern is strongly selected and any perturbation at the extremities of the front is rapidly damped. At low $Ca_e (< 0.02)$, some areas of the cellular pattern become unsteady, with propagating or oscillating cells and sometimes the disappearance and creation of cells (fig. 1*a*)). The size and the position of these disordered areas change with time, but this does not affect the amplitude of the cells. As we increase Ca_e, the average number of disordered cells in the pattern increases. At Ca_e larger than 0.03, the interface has everywhere lost its coherence, spatially and temporally. Although a mean wavelength still exists, we have reached the fully disordered state and the dynamic looks unchanged up to very large Ca_e values ($Ca_e > 5$).

In order to visualise the spatio-temporal behaviour of the front, we record the shape of the interface with a CCD camera on a Macintosh IIx computer. To avoid transient effects, we systematically waited 10 minutes in a given regime before any recording. Selecting one horizontal video line perpendicular to the cells and plotting this line at constant time intervals, we generate a spatio-temporal image of the type of fig. 1*b*). On such an image (764 pixels in space and 511 lines in time), the dark lines are the tracks of the oil walls between air cells.

As shown by fig. 1*a*) and 1*b*), ordered domains coexist in this transition with chaotic ones

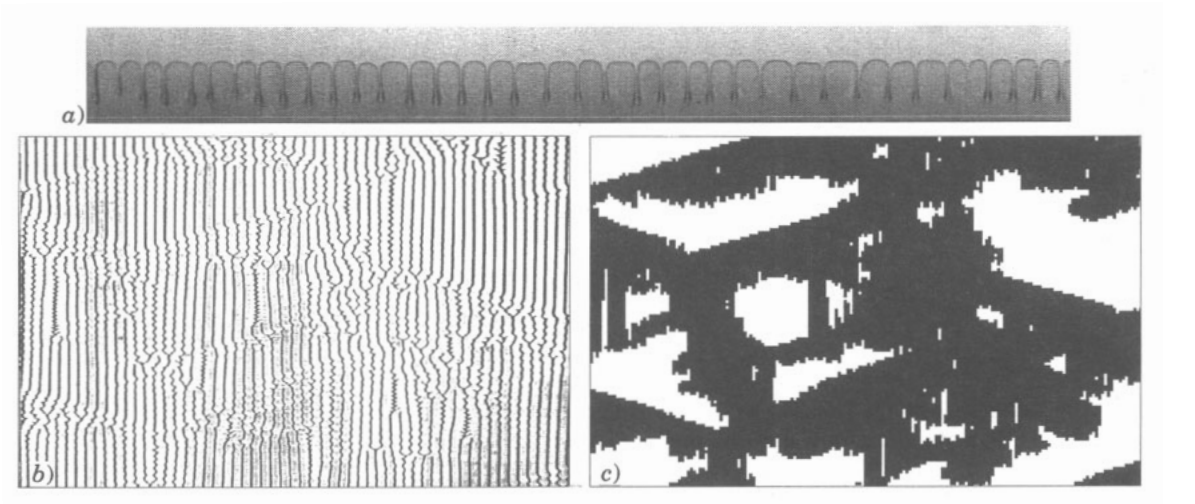

Fig. 1. – *a*) Photograph of a part of the interface for $Ca_i = 3$ and $Ca_e = 0.015$. Oil is above the air fingers. *b*) Temporal evolution of one horizontal line cutting the interface; 32 s elapse from top to bottom. *c*) Same picture as *b*) after the binarisation process described in the text (black represents chaotic domains, white the ordered ones).

in a dynamical equilibrium, the proportion of chaos depending only on Ca_e. We never observed any hysteretic behaviour of the dynamics. Another characteristic feature is that any unsteady area results from a contamination of an ordered domain by a nearby chaotic area (*i.e.* chaos never appears spontaneously isolated in the middle of an ordered domain but the reverse process, the spontaneous transition of a chaotic region to order, is often seen). Both characteristics are the attributes of a transition by STI.

In order to push further the comparison of our system with both model systems and other experimental systems exhibiting STI, we investigated the statistical properties of the distribution of the laminar domains. These clearly correspond in our system to the regions where the cells are steady. The best criterion for the discrimination of the laminar domains is therefore easy to implement: in the recorded spatio-temporal image, we subtract each line from the following one, erasing any steady track. This defines as chaotic any oil wall which moves by more than a tenth of a wavelength in a given time interval (about a tenth of a second). The exact value of this velocity criterion is not critical as the velocity of a moving wall is always large. Then we binarise the image in black and white, and filter the information below the wavelength size ([1]). Figure 1*c*) corresponds to fig. 1*b*) after this treatment.

Two things are worth noticing: firstly, the complement to the laminar regions is formed of strongly chaotic regions together with regions excited by the propagation of waves which form the contamination process for chaos. Secondly, our criterion is different from that used by other investigators of STI who used the setting of an amplitude threshold [3, 4] or of a wavelength threshold [4]. The former is not usable here as ordered and disordered cells have

([1]) This is done on the binarised picture by counting the number of black pixels in a square of 20 by 20 pixels. If this number is larger than a chosen value (typically 20 black pixels), the central square (4 by 4 pixels) is set to black, if not it is set to white. These numerical values of the filtering have been adjusted in order to give good results for the eyes. We checked that the statistics are not too sensible to the choice of the numerical values.

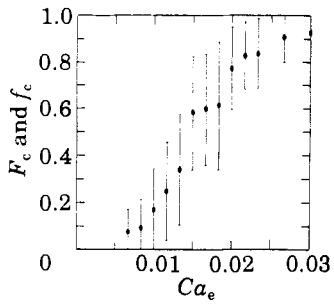

Fig. 2.

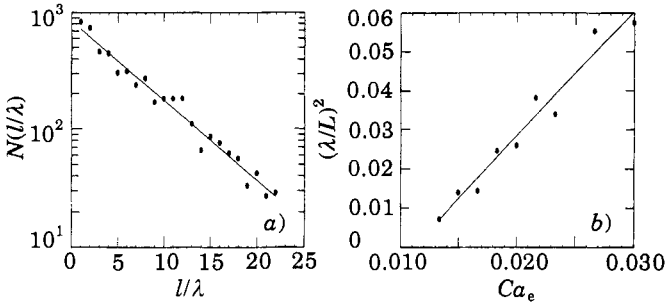

Fig. 3.

Fig. 2. – Mean chaotic fraction F_c (●) *vs.* external capillary number Ca_e for $Ca_i = 3$. Bars are not error bars on F_c, but standard deviation at one σ of the *instantaneous* chaotic fraction f_c.

Fig. 3. – *a*) Lin-log plot of the number $N(l/\lambda)$ of laminar domains of dimensionless width l/λ. This curve shows up the exponential behaviour (with $L = 6.38\lambda$) for $Ca_e = 0.0183$ (and $Ca_i = 3$). *b*) Evolution of the $(\lambda/L)^2$ *vs.* the external capillary number Ca_e. By a linear regression we found for the threshold of the STI regime $Ca_e = 0.011 \pm 0.001$.

the same amplitude. The latter does not distinguish between chaos and propagation and therefore gives results similar to ours.

As in ref. [2] and [3] we measured three macroscopic quantities for each given Ca_e and study their evolution along the transition. These quantities are

i) The instantaneous chaotic fraction, f_c, which corresponds to the ratio of the length of the pattern in the chaotic state to the total length of the pattern, and the mean chaotic fraction, F_c, which is the average of f_c on long time.

ii) The distribution of the width l of the ordered domains. Each histogram $N(l)$ results from the acquisition of approximately 2000 sample lines out of 20 min of recording.

iii) The distribution of the duration τ of ordered behaviour in a point. The histogram $N(\tau)$ results from the acquisition of 191 regularly spaced points during about 1000 s.

Figure 2 shows the increase of the mean chaotic fraction F_c with the control parameter Ca_e. The standard deviation on the instantaneous fraction f_c remains high all along the transition. This results from the strong intermittent behaviour of the front. In spite of this dispersion of f_c, the transition looks like an imperfect second-order phase transition.

For Ca_e in the range 0.015 to 0.03, the distribution $N(l)$ of the widths of the ordered domains can be fitted by a decreasing exponential (fig. 3*a*)). The *e*-folding distance L of the distribution of l is the characteristic width of the ordered areas. At high Ca_e, L is of the order of a few λ, the mean wavelength of the pattern. By decreasing Ca_e, L increases and finally diverges (*i.e.* it reaches the size of the whole front).

Figure 3*b*) shows the linear behaviour of $(\lambda/L)^2$ with Ca_e. From this plot we found the value of Ca_e where L diverges, $Ca_e = 0.011 \pm 0.001$. By analogy with the behaviour of the correlation length in a second-order phase transition, we call this value the threshold of STI transition.

Near this threshold, the distribution of the spatial width is no longer exponential and can be fitted by a decreasing power law (fig. 4). The exponent $\mu_s = 0.64 \pm 0.02$ can therefore be interpreted as a critical exponent of the STI transition.

Distributions in temporal duration $N(\tau)$ have a similar behaviour: at large Ca_e, they are well fitted by decreasing exponential with an *e*-folding time T. A linear regression on T^{-2}

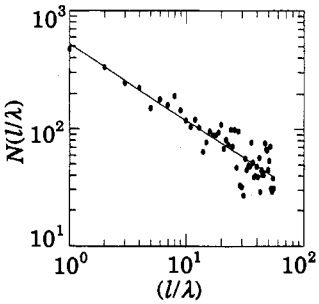

Fig. 4. – Log-log plot of the number $N(l/\lambda)$ of laminar domains of dimensionless width l/λ showing the power law behaviour (with exponent $\mu_s = 0.64 \pm 0.02$) for $Ca_e = 0.0117$ (and $Ca_i = 3$).

shows the divergence of T at a threshold $Ca_e = 0.010 \pm 0.001$ compatible with the previous value obtained for L. Near this value, the distribution of temporal duration is again a power law decay with a critical exponent $\mu_t = 0.61 \pm 0.02$.

So the STI transition behaves as a second-order transition with well-determined critical exponents. However, this transition is imperfect. Figure 2 shows that the chaotic fraction is non-zero below the above-determined threshold. An explanation can be found in the role of the boundaries. As discussed in ref. [6], the first disordered areas are created by perturbations localised at the ends of the interface. Below the STI threshold these perturbations propagate but are rapidly damped. In the vicinity of the threshold, there is less damping and perturbations (*i.e.* dilatation waves) travel all along the interface. Well above threshold, disturbances coming from the ends appear negligible in comparison to bulk disturbances generated by the deaths, births or collisions of cells. Nevertheless, neglecting this imperfect behaviour, we tried to fit the chaotic fraction F_c above threshold by a law in $(Ca_e - 0.010)^\beta$ in order to estimate the critical exponent β. Doing that we found the approximate value $\beta = 0.45 \pm 0.05$ close to the one-half exponent of a supercritical bifurcation.

The same transition has also been investigated for $Ca_i = 1.5$, but with smaller statistics. We found the same general behaviour for the STI transition and about the same exponents ($\mu_s = 0.60 \pm 0.05$, $\mu_t = 0.7 \pm 0.1$ and $\beta = 0.5 \pm 0.1$). This is worth noting because the local contamination processes are partly different. At this lower value of Ca_i the pairs of enlarged cells which maintain phase defects in time are not observed [6].

These results can be compared with the measurements done in other one-dimensional systems. Statistical studies of transitions to chaos by STI were done in simulations of a damped Kuramoto-Sivashinski equation [3] and in confined-convection experiments [4]. As in all these other cases, the transition in our system has the general characteristics of a second-order phase transition with exponential distributions far from threshold and power law distributions at threshold. It thus appears that the transition from order to chaos in extended one-dimensional systems exhibits common general properties defined as those of the spatio-temporal intermittency. However, the exponents of the power laws are different in the different systems. While we find $\mu_s = 0.64$, in convection experiments [4*a*, *b*] the exponents are $\mu_s = 1.9 \pm 0.1$ or $\mu_s = 1.6 \pm 0.2$, and in the Kuramoto-Sivashinski equation $\mu_s = 3.15$. As described above, the same criterion for the definition of the laminar regions could not be used in different systems. However, we do not believe this to be responsible for the difference in the value of the exponents. This difference should rather be ascribed to more fundamental differences between different systems.

In the convection experiments each of the elements is an oscillator with a characteristic

temporal frequency, while in our system it is a static cell. Correlatively the order and chaos are different: in convection the chaos affects mostly the amplitude and phase of the temporal oscillation, while in our experiment it affects the position (or spatial phase) of the cells and their existence. We can note that the Kuramoto-Sivashinski equation had been introduced either as the phase equation of coupled oscillators or to describe the shape of an unstable front in the physical space [13]. Though demonstrated in neither cases, this equation is thus probably a model for the phase dynamics in the convection experiments and for the front shape in our system.

The contamination process appears in our experiment [6] dominated by the propagation of dilatation waves also called parity-breaking waves which do not seem to be present in the other systems. This latter reason is in our opinion the most likely to be responsible for the non-universality of the exponents in the different systems.

* * *

We wish to acknowledge the help of H. THOMÉ and O. CARDOSO during the experiments.

REFERENCES

[1] CROSS M. C. and HOHENBERG P. C., *Pattern formation outside of equilibrium*, to appear in *Rev. Mod. Phys.*

[2] KANEKO K., *Prog. Theor. Phys.*, **74** (1985) 1033.

[3] CHATÉ H. and MANNEVILLE P., *Phys. Rev. Lett.*, **58** (1987) 112.

[4] *a*) CILIBERTO S. and BIGAZZI P., *Phys. Rev. Lett.*, **60** (1988) 286; *b*) DAVIAUD F., DUBOIS M. and BERGÉ P., *Europhys. Lett.*, **9** (1989) 441; DAVIAUD F., BONNETTI M. and DUBOIS M., *Phys. Rev. A*, **42** (1990) 3388; *c*) WILLAIME H., CARDOSO O. and TABELING P., *Spatio-temporal intermittency in lines of vortices*, to appear in *Phys. Rev. E.*

[5] RABAUD M., MICHALLAND S. and COUDER Y., *Phys. Rev. Lett.*, **64** (1990) 184.

[6] MICHALLAND S. and RABAUD M., *Physica D*, **61** (1993) 1097.

[7] HAKIM V., RABAUD M., THOMÉ H. and COUDER Y., in *New Trends in Non-linear Dynamics and Pattern Forming Phenomena*, edited by P. COULLET and P. HUERRE (Plenum Press, New York, N.Y.) 1990, p. 327.

[8] RUSCHAK K. J., *Ann. Rev. Fluid Mech.*, **17** (1985) 65.

[9] RABAUD M. and HAKIM V., in *Instabilities and Nonequilibrium Structures III*, edited by E. TIRAPEGUI and W. ZELLER (Kluwer Academic Publishers) 1991, p. 217.

[10] CUMMINS H., FOURTUNE L. and RABAUD M., *Successive bifurcations in directional viscous fingering*, preprint (1992).

[11] RABAUD M., COUDER Y. and MICHALLAND S., *Eur. J. Mech. B*, **10**, 2 Suppl. (1991) 253.

[12] SIMON A. J., BECHHOEFER J. and LIBCHABER A., *Phys. Rev. Lett.*, **61** (1988) 2574; FAIVRE G., DE CHEVEIGNÉ S., GUTHMANN C. and KUROWSKI P., *Europhys. Lett.*, **9** (1989) 779.

[13] KURAMOTO Y. and TSUZUKI T., *Prog. Theor. Phys.*, **55** (1976) 356; SIVASHINSKY G. I., *Acta Astron.*, **4** (1977) 1177.